Remote activation of aerolysin nanopore for high performance genetic detection using a pH taxis-mimicking mechanism

Yong Wang, Kai Tian, Xiao Du, Rui-Cheng Shi and Li-Qun Gu

Supplementary Information

Table S1-S2

Figure S1-S12

Supplementary Information S1-S3

Table S1. Sequences of DNAs and RNA targets used in the study

Target	Sequence
D5 (DNA)	5′-TGGTT-3′
D16 (DNA)	5′-TCCCTACCACGATTAT-3′
D30 (DNA)	5′-ATCATCATTGAGGTAGTAGGTTGTGTGGTT-3′
miR-155 (microRNA)	5′-UUAAUGCUAAUCGUGAUAGGGG-3′

Table S2. pKa of amino acid residue and nucleotide base analytes

Analyte	pKa	Protonation	Position
Arginine	12.5	$R \rightarrow RH^+$	
Lysine	10.5	$K \rightarrow KH^+$	
Aspartic Acid	3.9	$D^- \rightarrow DH$	
Glutamic Acid	4.1	$E^- \rightarrow EH$	
Histidine	6.1	$H \rightarrow HH^+$	
Cysteine	8.0	$C^- \rightarrow CH$	
Tyrosine	10.1	$Y^- \rightarrow YH$	
Adenine	3.5	$A \rightarrow AH^+$	N3
Cytosine	4.2	$C \rightarrow CH^+$	N3
Guanine	2.1	$G \rightarrow GH^+$	N7
	9.2	$G^- \rightarrow GH$	
Thymine	9.9	$T^- \rightarrow T$	N1
Uracil	10.0	$U^- \rightarrow U$	N3
Phosphate	1.0	$Pi^- \rightarrow Pi$	N3
	6.3	$Pi^{2-} \rightarrow Pi^-$	

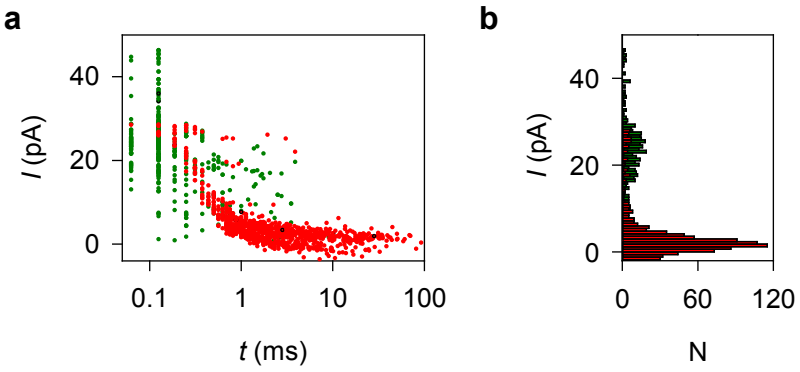

Figure S1. Characterization of DNA target D16-generated current blocks. **a.** Block current-duration scattering plot at +80 mV; **b.** Current amplitude histogram constructed using data in the scattering plot. DNA was presented in the *cis* solution. Data in green is for pH7.4 on both sides, and data in red is for *trans* pH3.4 with *cis* pH remaining 7.4.

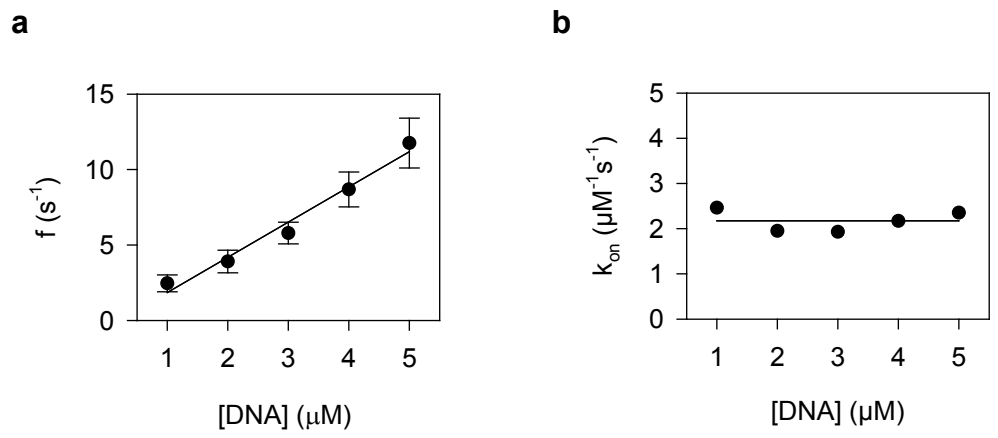

Figure S2. Block frequency (capture rate, *f*) and capture rate constant (k_{on}) as the functions of DNA concentration ([DNA]). Recording solutions contained 1 M KCl and 10 mM Tris. DNA D16 of various concentrations was presented in the *cis* solution at pH7.4, and *trans* pH=3.2. Data was collected from current traces recorded at +60 mV. **a.** *f*–[DNA] curve. *f* is proportional to [DNA]; **b.** k_{on}–[DNA] curve. k_{on} was obtained from $k_{on}=f/[DNA]$, so k_{on} remain a constant. The result indicates that the blocking events observed at low *trans* pH occur more frequent as DNA concentration increased, suggesting that the observed blocks are produced by D16.

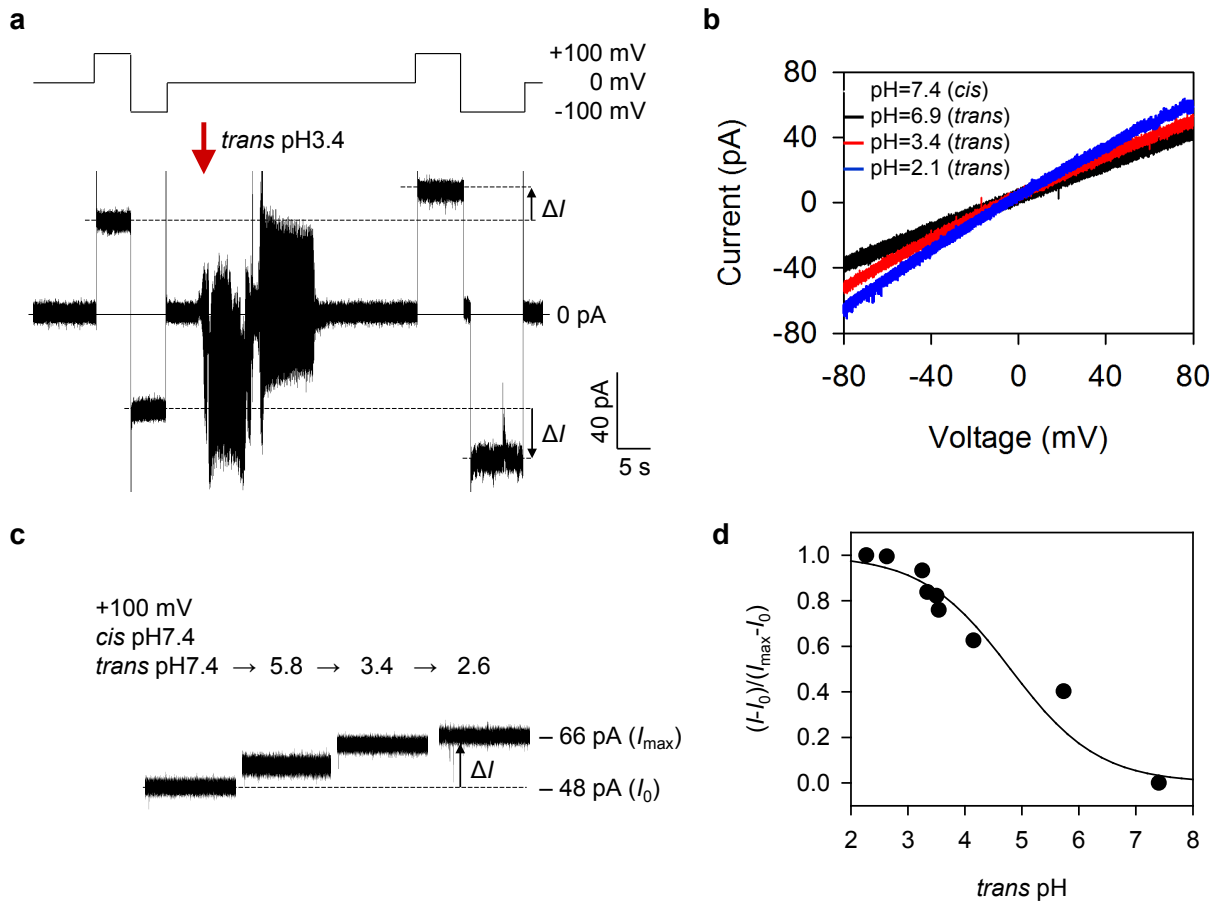

Figure S3. *Trans* pH-dependent current trace of aerolysin in the absence of DNA. There was no full current blocks observed at voltages smaller than +100 mV. In addition to activation of aerolysin for DNA capturing, the acidity also increased the conductance of the aerolysin pore alone. This effect has been found for the α-hemolysin pore and has been explained as the result of protonation, which concentrates counter-ions (anions) and increases the overall conductance of the pore[1]. **a.** A continuous current trace showing that the current amplitude of the aerolysin pore increases as the *trans* pH was lowered from 7.4 to 3.4, while the *cis* solution remained neutral pH (7.4); **b.** Current-voltage curves (I-V ramps) for *trans* pH=6.9, 3.4, and 2.1, showing the increase of the aerolysin conductance by lowing *trans* pH; **c.** Current traces showing the

continuous increase of the pore conductance from 48 pA to 66 pA at +100 mV as *trans* pH was lowered from 7.4 to 2.6; **d.** Fraction of current increase as a function of *trans* pH. The relation can be fitted with a sigmoidal curve, $(I - I_0)/(I_{max} - I_0) = 1/(1 + 10^{pH - pH_{0.5}})$, where I_0 and I are open currents of aerolysin in neutral (pH=7.4) and acidic (pH<7.4) *trans* solutions (*cis* pH=7.4). I_{max} is the maximal current that can be obtained when lowering *trans* pH (*trans* pH2.1). $pH_{0.5}$ is the fitted pH values at which current is increased to 50% of I_{max}. This result indicates that in the absence of DNA, lowering *trans* pH does not generate current blocks, but can monotonically increase the open pore current, due to protonation of the pore lumen.

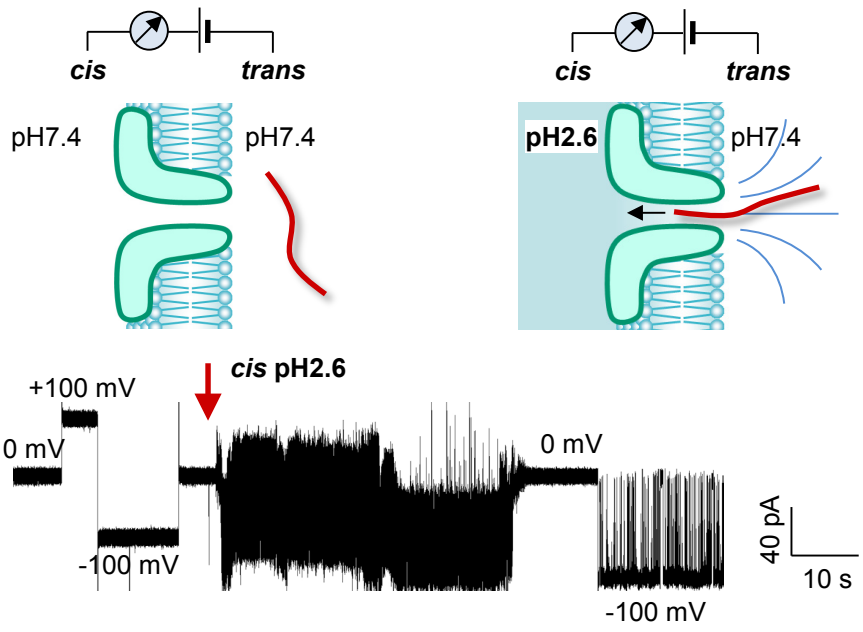

Figure S4. Activation of aerolysin by acidic solution on one side to capture DNA from the other side capture and translocation. Model (up) and current trace (bottom) showing that DNA D16 (1 μM) presented on *trans* side cannot be captured in the aerolysin pore when both *cis* and *trans* solutions were at pH7.4 (left), and the *trans* DNA can immediately generate a large number of current blocks when the *cis* solution was changed to pH3.4 while *trans* solution remained pH7.4 (right). Red arrow marks the time point when *cis* pH was changed from 7.4 to 2.6.

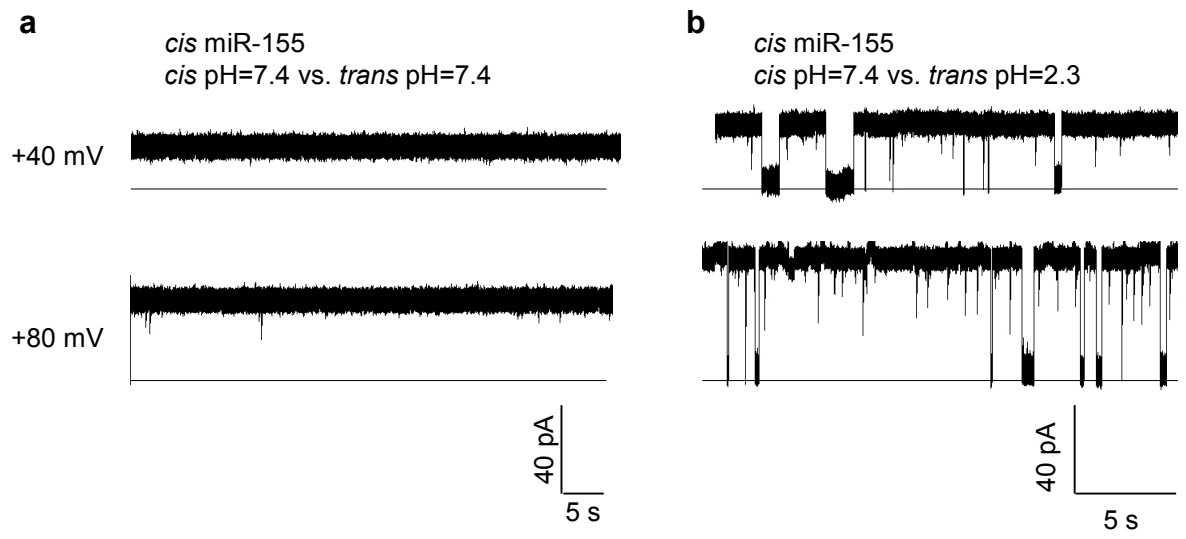

Figure S5. Translocation of microRNA miR-155 from *cis* side of the aerolysin pore by lowering *trans* pH. 100 nM of miR-155 (Table S1) was presented in the *cis* chamber. **a)** Current traces showing that, similar to DNA, *cis* RNA did not produce blocks at +40 and +80 mV in symmetric neutral pH7.4 solution; **b)** Current traces showing that, when *trans* pH was lowered to 2.3 (*cis* pH remained 7.4), there generated a large number of RNA blocks at low voltage. The block duration τ was 810±120 ms at +40 mV, and was shortened to 310±90 ms when voltage was increased to +80 mV, suggesting that RNA can be captured and translocate through the aerolysin pore under small voltage. Both durations are longer compared with DNA translocation at the same voltages (Fig. 2), probably due to the need for unfolding of RNA while translocating through the narrow pore. The RNA capture rate k_{on} was 2.1±0.4 $\mu M^{-1}s^{-1}$ at +40 mV, and k_{on} increased to 4.8±0.6 $\mu M^{-1}s^{-1}$ at +80 mV, representing high capture efficiency at low voltages.

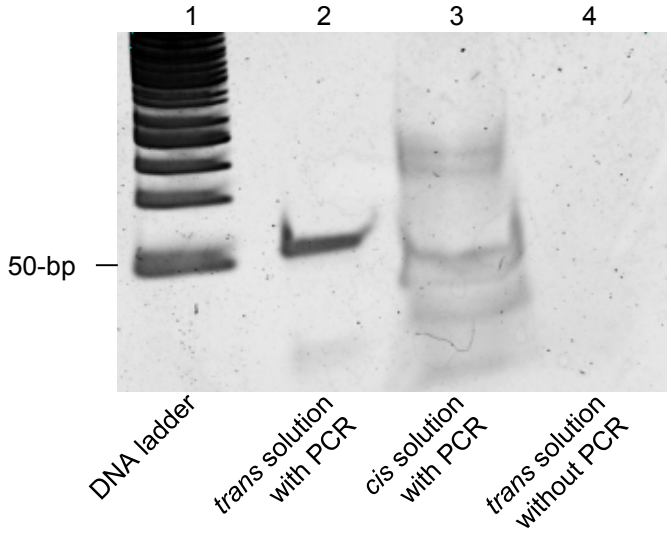

Figure S6. PCR experiment for examining DNA translocation through the pH-activated aerolysin pore. 10 μM of 50-nt DNA was presented in the *cis* solution. The sequence of the DNA is GGT GAA AGC ATT TCC CAT TCA TTG TCA TGG GTA ACT GCA TCC GGG CCA GC. Both *cis* and *trans* solutions contained 1 M KCl and 10 mM Tris, with *cis* pH=7.4 and *trans* pH=3.1 (titrated with HCl). About 20 aerolysin pores were formed and simultaneously recorded at +50 mV (*cis* side grounded) for about 1 hour. The membrane remained stable under this condition throughout the recording. After electric monitoring for DNA translocation, the *trans* solution was titrated to pH7.4 using KOH. 10 μL of *trans* or *cis* solutions was mixed with 1 μl of 10μM each primer, 2μL Green Master Mix (Promega) and ddH_2O to 100 μL for PCR. The sequences of the forward and reverse primers are GGT GAA AGC ATT TCC CAT TCA and GCT GGC CCG GAT GCA GTT, respectively. The PCR thermal cycle condition was 94 ^oC for 2 min, 40 cycles of 94 ^oC for 30s, 55 ^oC for 30s, and 72 ^oC for 30s, and 72 ^oC for 5 min for finalization. The PCR products for the *trans* (Lane-2) and *cis* solution (Lane-3) as well as the *trans* solution without PCR (Lane-3) were examined using 12% DNA polyacrylamide gel

electrophoresis as illustrated. The 50-bp PCR amplicon is identified from the *trans* solution, verifying the translocation of D50 through the aerolysin pore from *cis* to *trans* side. Lane-3 contains several bands, probably due to the high concentration of the single strand DNA added from *cis* side. Because of the low concentration of the translocated single strand, no band can be identified without PCR in Land-4.

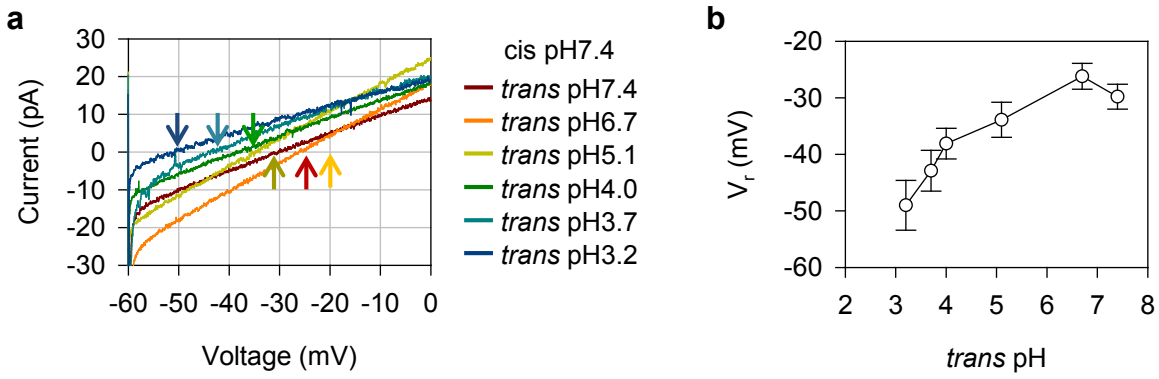

Figure S7. *Trans* pH-regulated ion selectivity of the aerolysin pore. **a.** Current-voltage (I−V) curves of aerolysin at various *trans* pH. The *cis* solution retained pH7.4. Arrows in different colors mark the reverse potential (V_r), i.e. the voltages that give zero-current (I=0), in different I-V curves; **b.** Variation of V_r as the function of *trans* pH. As the *trans* pH was lowered from 7.4 to 6.7, 5.1, 4.0, 3.7, 3.2, V_r trended to be more negative, from −29, to −26, −34, −38, −43, and −49 mV. The negative polarity of V_r indicates that aerolysin is an anion (Cl^-)-selective pore. Lowering *trans* pH can greatly enhance the anion selectivity. The ion selectivity is measured by the K^+/Cl^- permeability ratio P_+/P_-, which was calculated using the GHK equation. P_+/P_- values at various *trans* pH are shown in Fig. 3b in the main text.

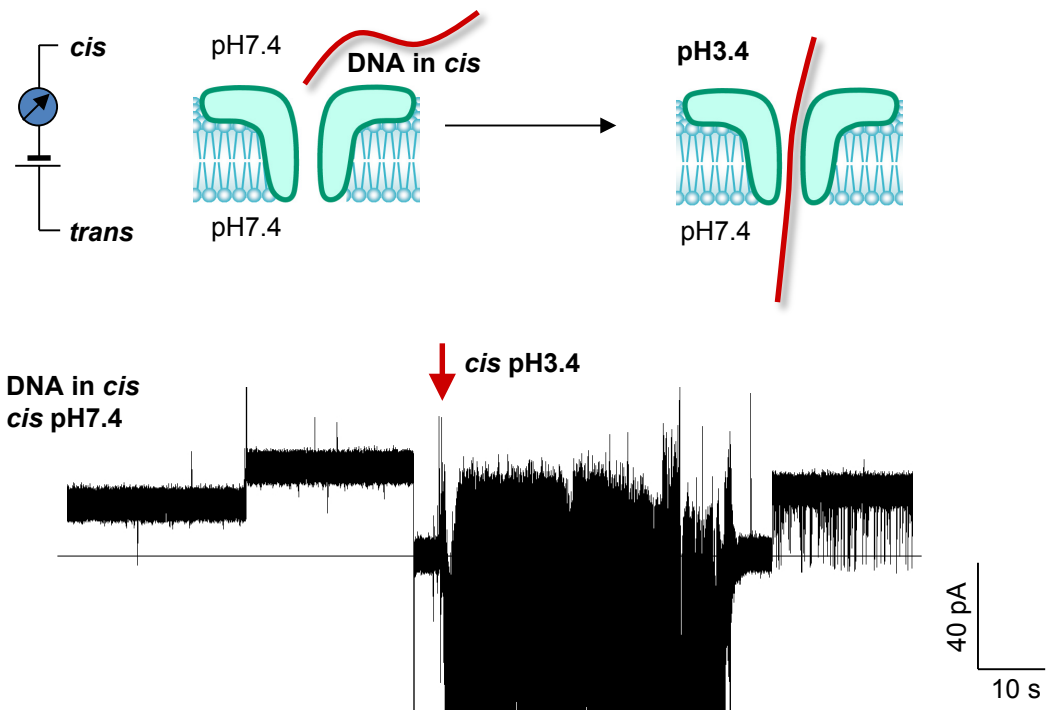

Figure S8. Continuous current trace showing DNA capture and translocation from *cis* side of the aerolysin pore by lowering the pH in the *cis* solution. 1 μM DNA D16 (Table S1) was presented in the *cis* solution. This trace was for two independent pores. DNA did not block the pore at pH7.4 in both *cis* and *trans* solutions, whereas when *cis* pH was lowered to 3.4, DNA produced a large number of blocks from the *cis* side, with one or two pores.

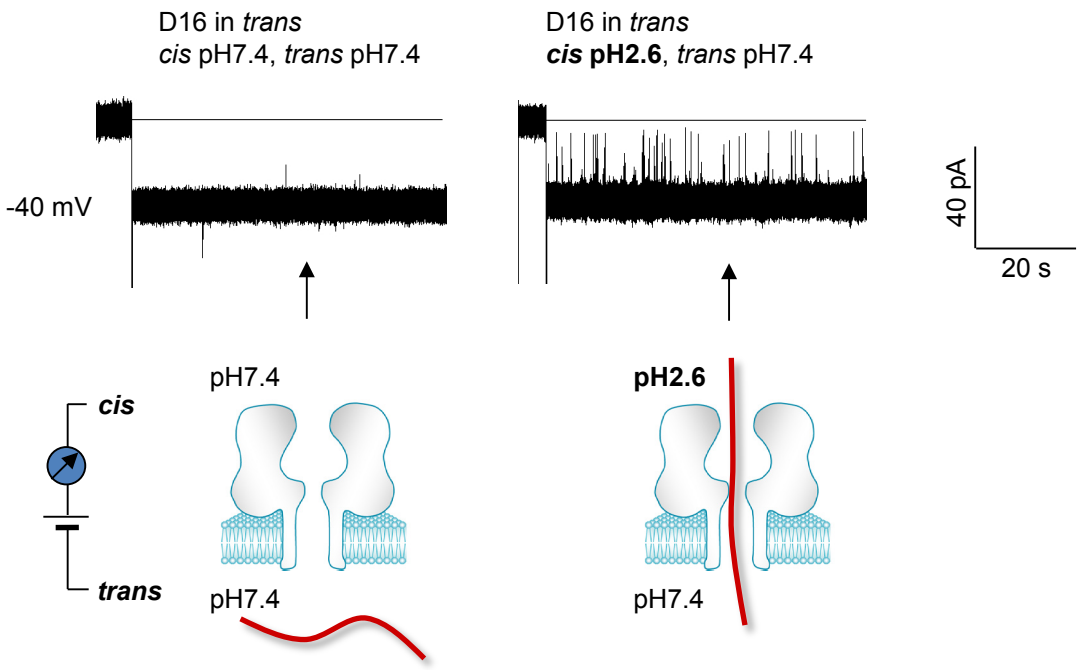

Figure S9. Continuous current trace showing DNA capture and translocation from *trans* side of the α-hemolysin pore by lowering the pH in the *cis* solution. 1 μM DNA D16 (Table S1) was presented in the *trans* solution. It has been known and as shown in the trace, *trans* DNA did not block the pore at −40 mV when both *cis* and *trans* solutions were pH7.4. When *cis* pH was lowered to 2.6, a large amount of DNA blocks from the *trans* side were observed, as illustrated by model below the trace. This result suggests that similar to the aerolysin pore, the α-hemolysin pore can be activated to allow DNA translocation from *trans* side by lowering pH on the other side, in the *cis* solution.

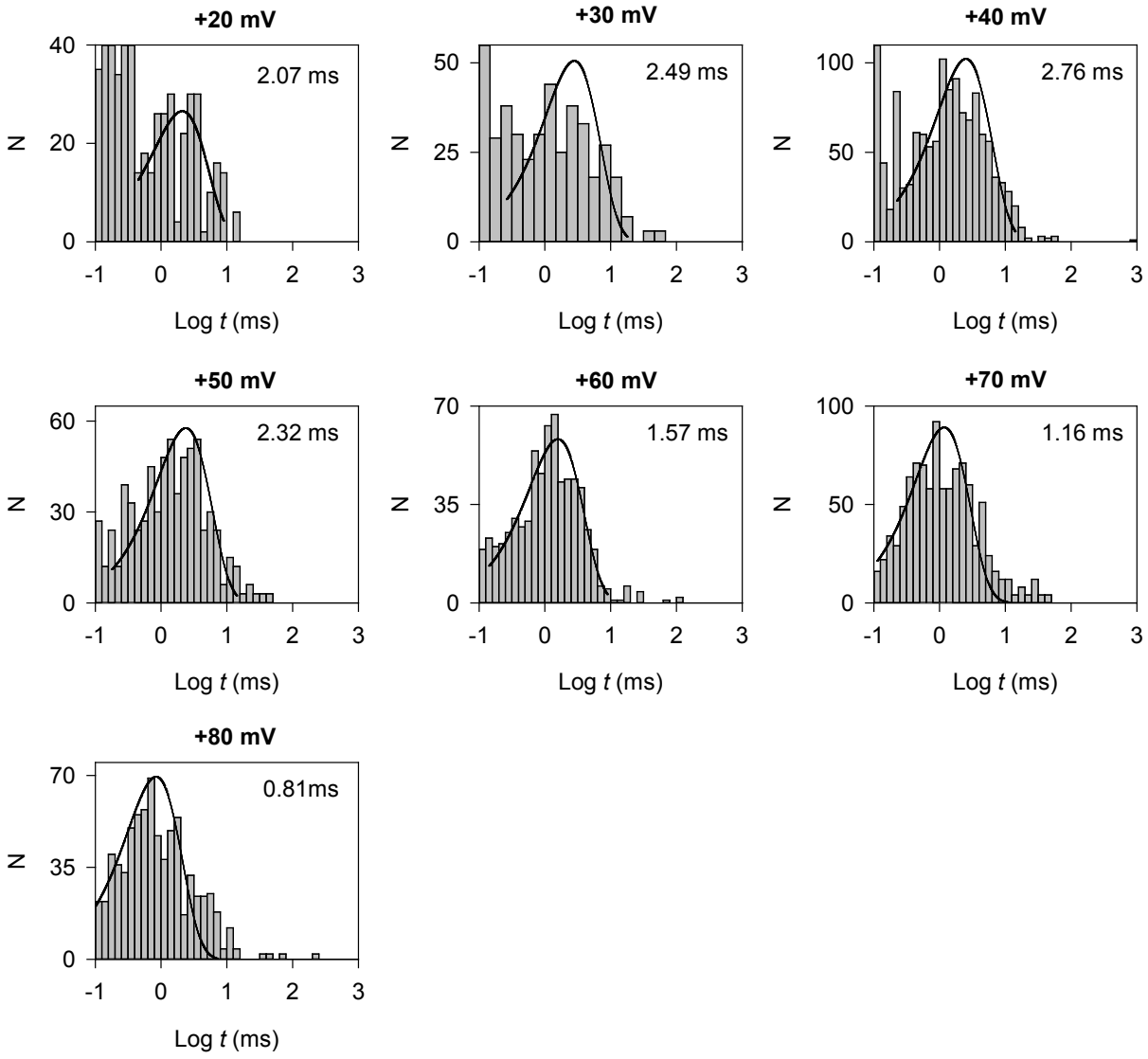

Figure S10a. Histograms of block duration histograms for translocation of D16 through the aerolysin pore at various voltages. 1 μM DNA was presented in the *cis* solution. *cis* pH=7.4 versus *trans* pH=3.4. Nanopore current blocks were recorded at +10, +20, +30, +40, +50, +60, +70, and +80 mV.

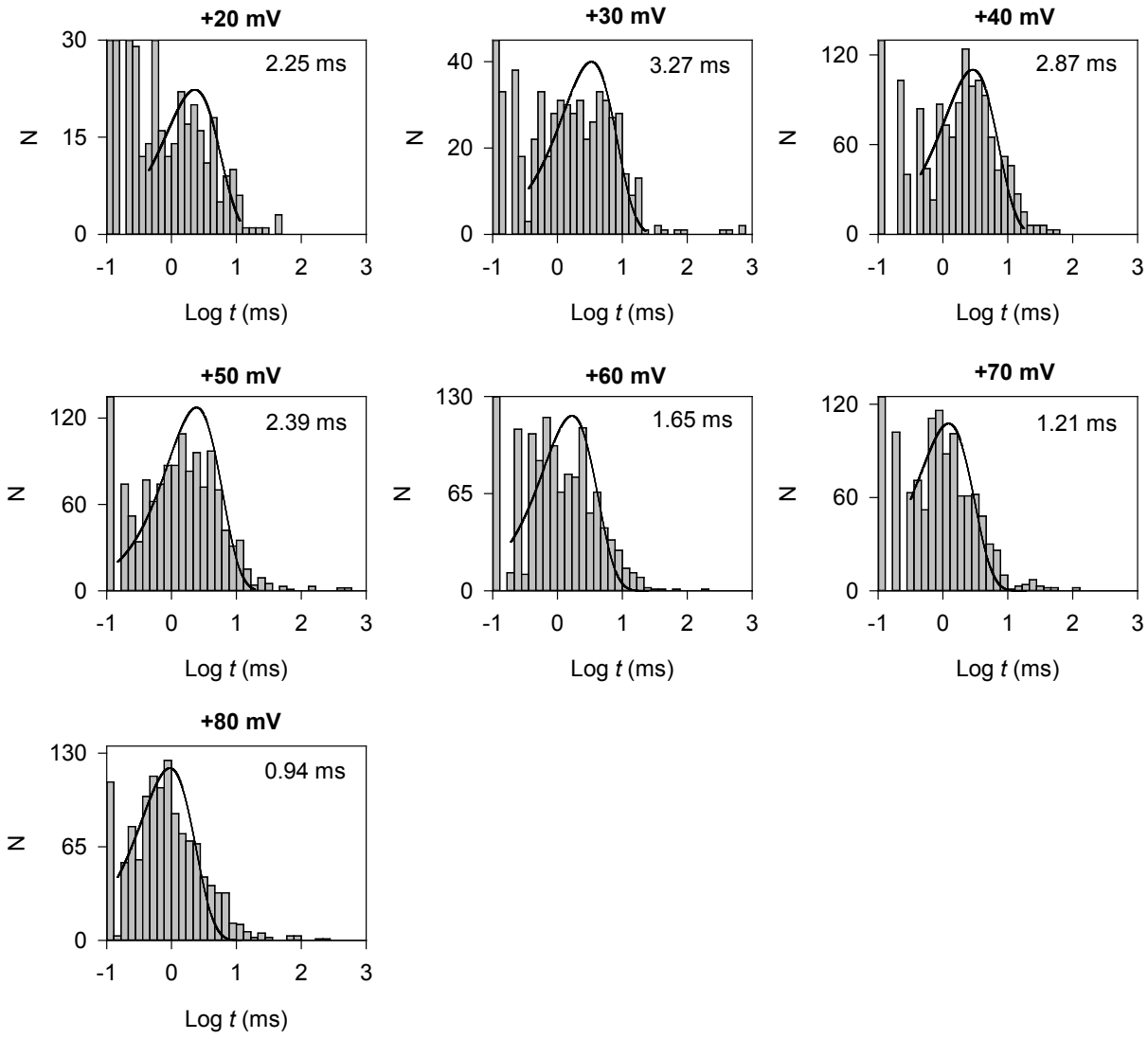

Figure S10b. Histograms of block duration histograms for translocation of D16 through the aerolysin pore at various voltages. 1 μM DNA was presented in the *cis* solution. *cis* pH=7.4 versus *trans* pH=3.2. Nanopore current blocks were recorded at +10, +20, +30, +40, +50, +60, +70, and +80 mV.

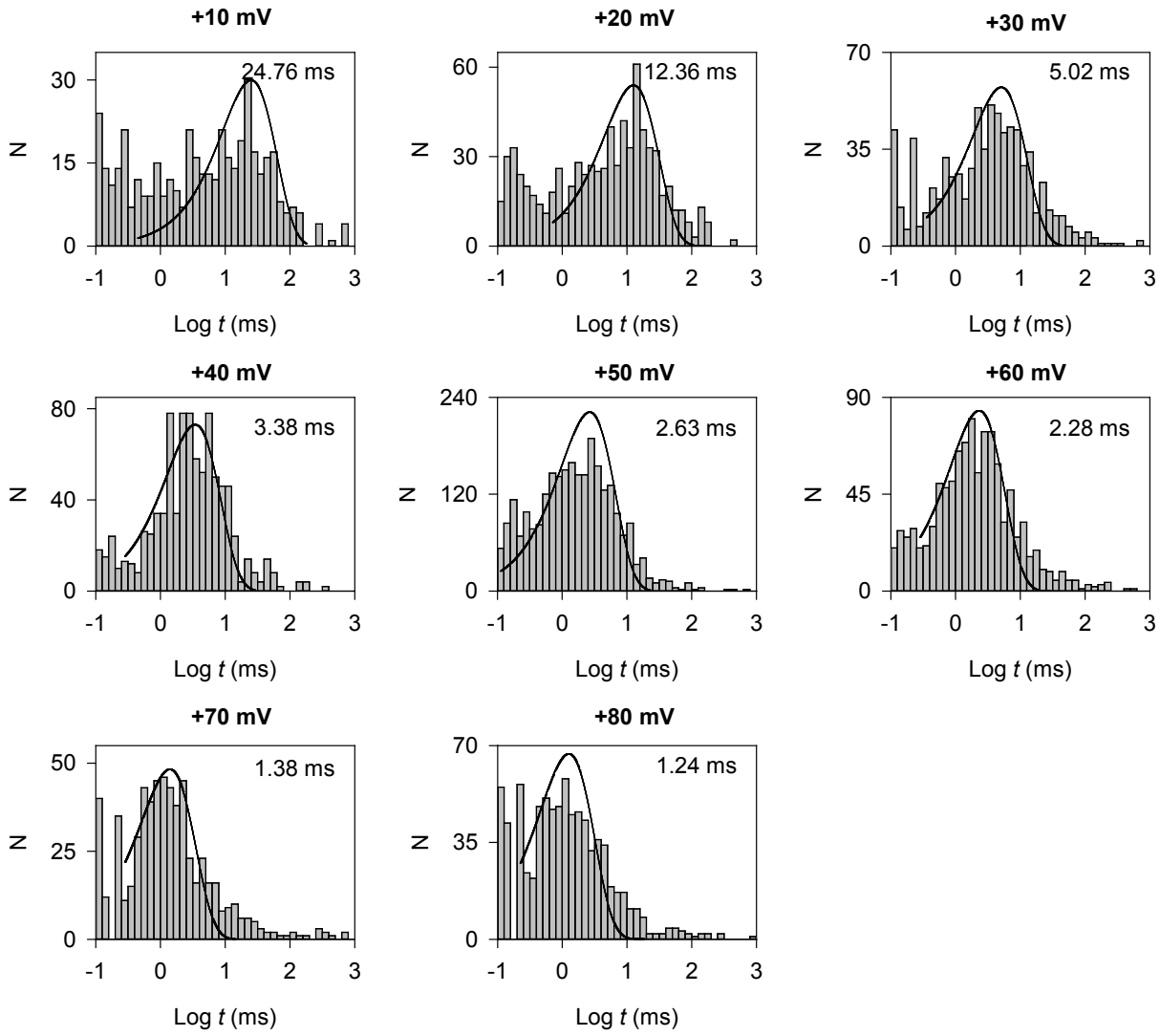

Figure S10c. Histograms of block duration histograms for translocation of D16 through the aerolysin pore at various voltages. 1 μM DNA was presented in the *cis* solution. *cis* pH=7.4 versus *trans* pH=2.6. Nanopore current blocks were recorded at +10, +20, +30, +40, +50, +60, +70, and +80 mV.

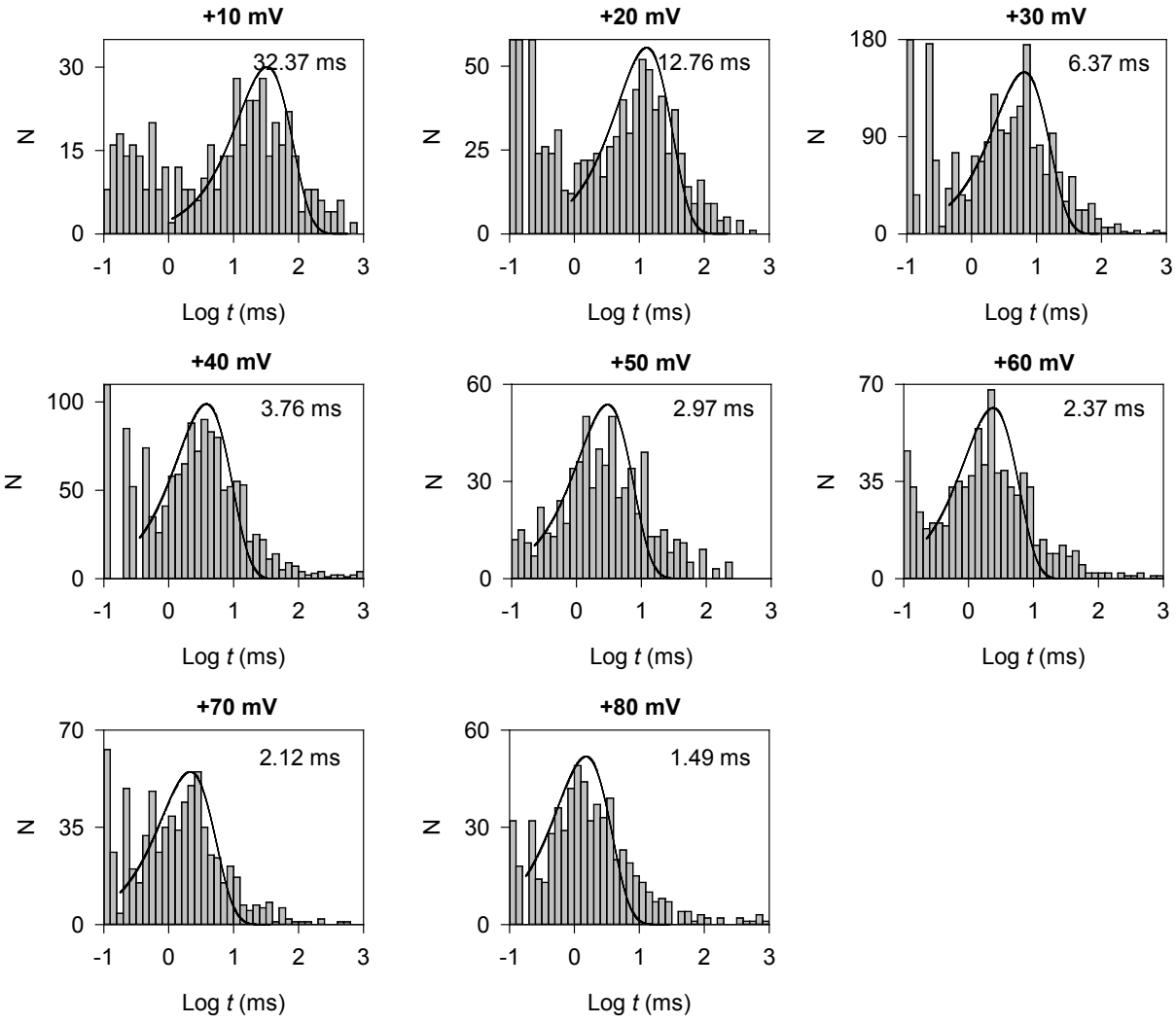

Figure S10d. Histograms of block duration histograms for translocation of D16 through the aerolysin pore at various voltages. 1 μM DNA was presented in the *cis* solution. *cis* pH=7.4 versus *trans* pH=2.3. Nanopore current blocks were recorded at +10, +20, +30, +40, +50, +60, +70, and +80 mV.

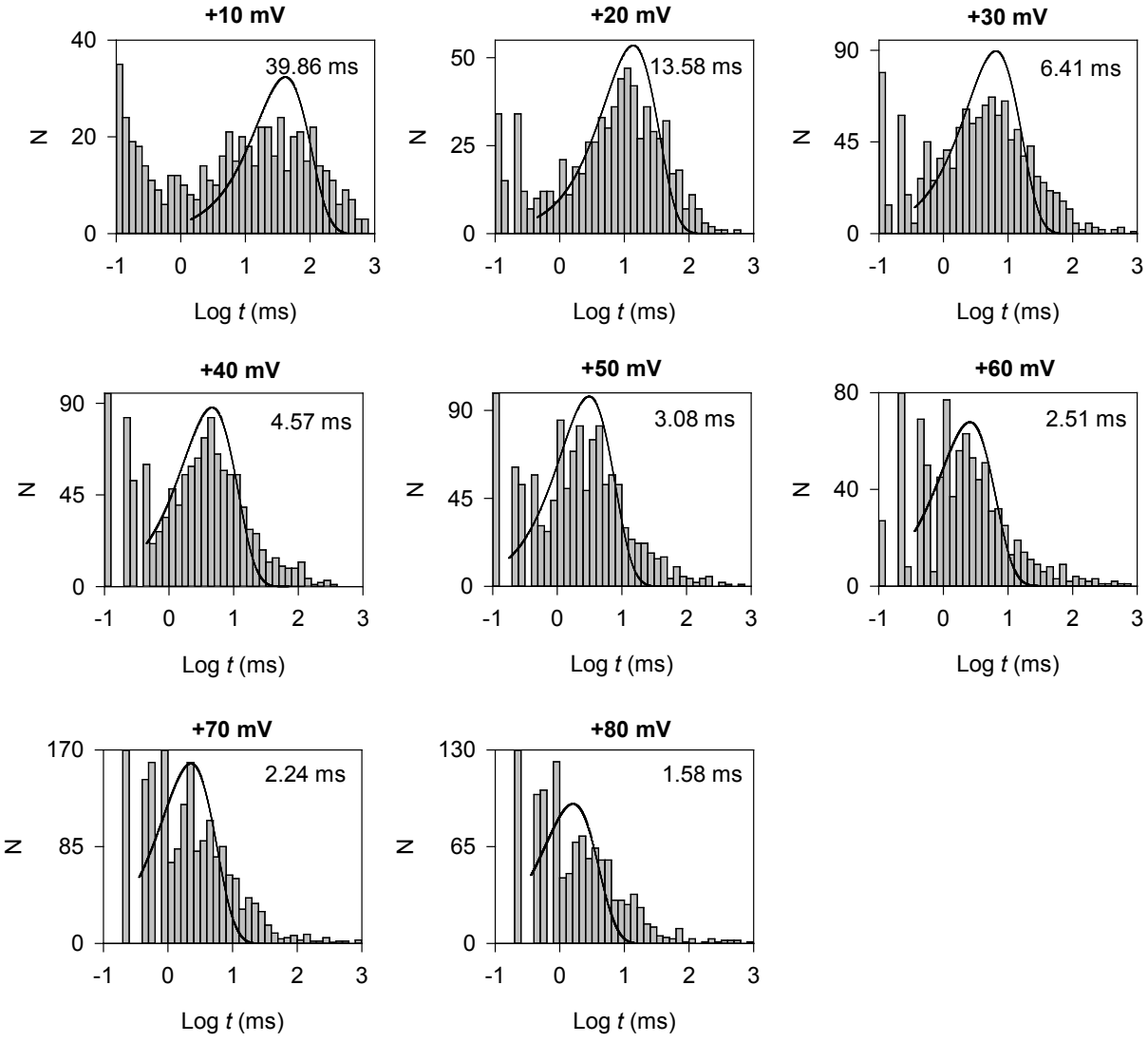

Figure S10e. Histograms of block duration histograms for translocation of D16 through the aerolysin pore at various voltages. 1 μM DNA was presented in the *cis* solution. *cis* pH=7.4 versus *trans* pH=2.1. Nanopore current blocks were recorded at +10, +20, +30, +40, +50, +60, +70, and +80 mV.

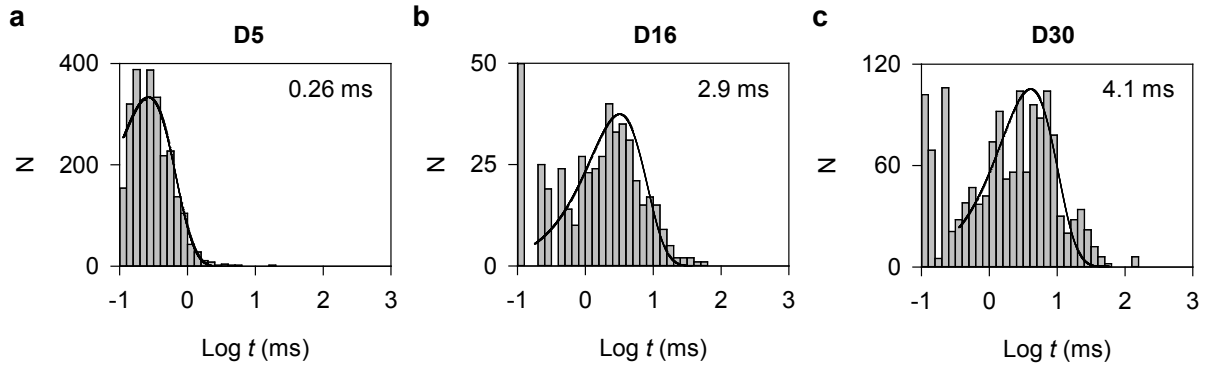

Figure S11. Histograms of block duration for translocation of D5 (a), D16 (b) and D30 (c) through the aerolysin pore. 1 μM DNA was presented in the *cis* solution. *cis* pH=7.4 versus *trans* pH=3.2. Nanopore current blocks were recorded at +40 mV.

S1. Diffusion− versus barrier−limited DNA capture by the aerolysin pore

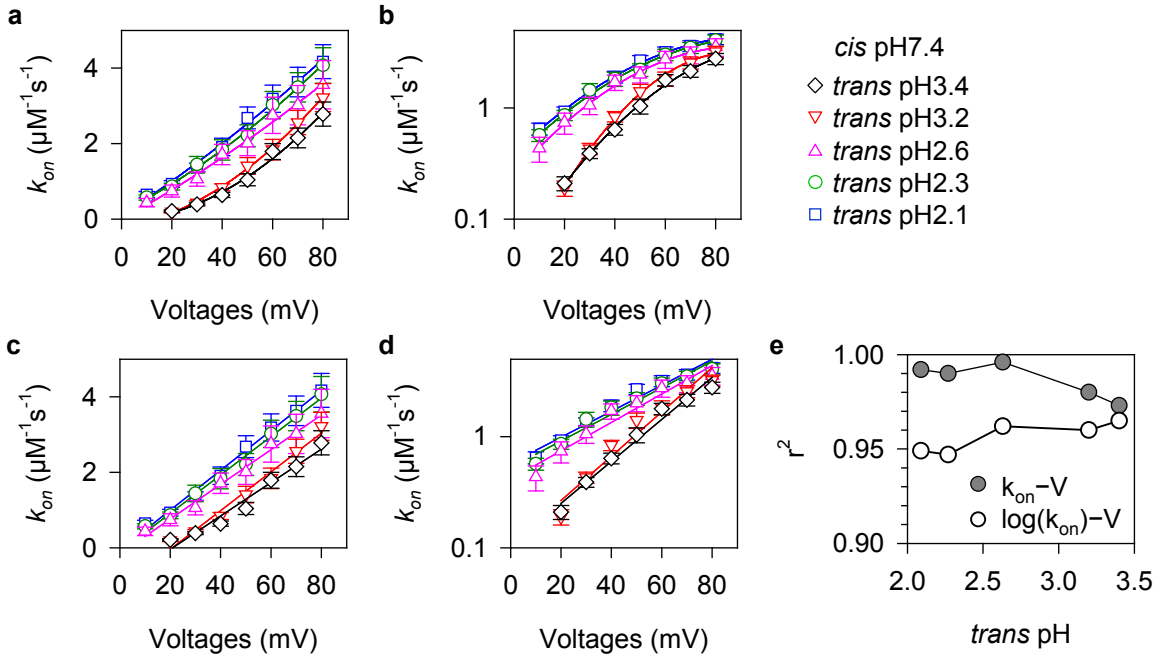

Figure S12. a-d, k_{on}−V with linear k_{on} scale (a and c) and log k_{on} scale (b and d) at different acidic *trans* pH and their fittings by quadratic (a and b) and linear (c and d) equations. **e.** Comparison of regression coefficients (r^2) for linear regression fitting of k_{on}−V curves in the linear k_{on} scale (c) and in log k_{on} scale (d).

We use r^2 to evaluate the fitting quality. The result of r^2 in panel e indicates that **1)** r^2 for linear k_{on} scale (c) is higher than that for log k_{on} scale (d) for all *trans* pH we tested, and **2)** as *trans* pH was lowered from 3.4 to 2.1, r^2 for linear k_{on} scale (c) increased from 0.973 to 0.992, while r^2 for log k_{on} scale (d) decreased from 0.960 to 0.949. This result suggests that **1)** k_{on}−V curves with linear k_{on} scale (c) can obtain better linear fitting than curves with log k_{on} scale (d). Therefore the k_{on}−V correlation can be considered as two components. It more approximates to a linear correlation (k_{on}~V) than an exponential correlation (k_{on}~exp(V)) as *trans* pH decreases.

Studying the voltage (V)-dependence of the capture rate (k_{on}) can help to understand the nature of the capture procedure. In a capture event, a DNA molecule first migrates from the bulk solution to the pore opening. This is a diffusive step biased by an electric field outside the pore entrance[2-4]. It is characterized by a linear k_{on}−V relation[2, 3, 5]. Next, the DNA is threaded into the pore for translocation, a step that needs to overcome an energy barrier due to the nanopore confinement of DNA end and/or DNA−pore interactions[2, 3, 5]. This barrier-limited capture allows k_{on} to be exponentially changed with the voltage (k_{on}~exp(V))[2, 3, 5]. The DNA capture by aerolysin can be considered as both voltage-biased diffusion-limited and barrier-limited procedures, but diffusion plays a more dominative role as *trans* pH decreases, due to better linear fitting of the k_{on}−V curves as *trans* pH decreases. This result implies that lowering *trans* pH can decrease the barrier for capturing DNA from the *cis* entrance.

S2. Nucleic acid protonation and charge evaluation

Protonation of a chemical group results in addition of charge. This process can be described quantitatively. When a residue R is protonated to RH^+, i.e. $R+H^+ \leftrightarrow RH^+$, the probability of the residue in the protonated state (RH^+), P_{RH} (varying between 0~1), can be calculated from the Henderson–Hasselbalch equation,

$$P_{RH} = 1/(1 + 10^{\mathrm{pH-pKa}}) \qquad \text{S1}$$

where pKa is the pH value at which P_{RH}=50%, i.e. the amount of protonated and unprotonated molecules are equal. P_{RH} can be considered as the addition of a fractional protonation charge to the residue R. For example, when pH=pKa, PRH=50%, the residue is half-protonated, thus the protonation charge would be +0.5*e*. Based on the Henderson–Hasselbalch equation (Eq. S1), the protonation charge at different pH can be calculated as below

pH vs pKa	P_{RH}	Protonation charge
pH=pKa−1	+0.91	+0.91*e*
pH=pKa−0.5	+0.76	+0.76*e*
pH=pKa−0.2	+0.61	+0.61*e*
pH=pKa−0	+0.50	+0.50*e*
pH=pKa+0.2	+0.39	+0.39*e*
pH=pKa+0.5	+0.24	+0.24*e*
pH=pKa+1	+0.09	+0.09*e*

For pH<pKa−1, the protonation charge is >+0.91*e*, the residue at this pH can be considered as fully protonated; For pH>pKa+1, the protonation charge is <+0.01*e*, the residue can be considered as not protonated.

In our current study, the middle point of capture rate increase is around pH3.2 (Fig. 3b). At this pH, the phosphate in DNA (pKa is close to 1) cannot be protonated (pH>pKa+1). Thus the charge of phosphate remains −1*e*. For nucleosides, Guanine (pKa=2.1) cannot be protonated at pH3.2 (pH>pKa+1); Thymine (pKa=9.9) and Uracil (pKa=10) have already been protonated at neutral pH. Therefore pH3.2 will not add more charges to both bases. In contrast, Adenine (pKa=3.5) and Cytosine (pKa=4.2) can be protonated at pH3.2. According to the Henderson–Hasselbalch equation (Eq. S1), the protonation charge is +0.57*e* for Adenine and +0.91*e* for Cytosine. Therefore DNA still carry negative charge at pH3.2, but the charge amount is reduced compared to that at neutral pH. For example, in the target D16 (TCCCTACCACGATTAT), the phosphate's negative charge remains −16e. The protonation of the six C bases produces +6×0.91e=+5.46*e*, and protonation of the four A bases yields +4×0.57e=+2.28*e*. Thus the overall charge is reduced to (−16+5.46+2.28)*e*=−8.26*e*. Charge reduction on DNA could be a possible factor for prolonged translocation time in acidic *trans* pH (from pH3.4 to 2.1).

S3. Supplementary Methods

Aerolysin protein. The proaerolysin was purchased from Aerohead Sci Ltd (Saskatoon, SK). 2 μM proaerolysin was incubated with trypsin (1μg/ml final concentration in the mixture) for 1.5 hour at room temperature to from aerolysin, then was stored at −80 °C.[6] Through this process, aerolysin can form protein pore in the lipid bilayer

Single-channel recordings. The electrophysiology setup and nanopore experimental methods have been well-documented[7]. Briefly, the recording apparatus was composed of two chambers (*cis* and *trans*) that were partitioned with a Teflon film. The planar lipid bilayer of 1,2-diphytanoyl-sn-glycerophosphatidylcholine (Avanti Polar Lipids) was formed spanning a 100-150 μm hole in the center of the partition. The aerolysin protein can be inserted in the lipid bilayer to form a protein pore. Both *cis* and *trans* chambers were filled with symmetrical 1 M salt solutions (KCl) buffered with 8 mM K_2HPO_4 and 2 mM KH_2PO_4 and titrated with HCl to specific pH values, including pH7.4, 3.4, 3.2, 2.6, 2.3 and 2.1. All saline solutions were filtered with 0.22 μm before the experimental use. Single-channel currents were recorded with an Axopatch 200A patch-clamp amplifier (Molecular Device Inc., former Axon Inc.), filtered with a built-in 4-pole low-pass Bessel Filter at 5 kHz, and acquired with Clampex 9.0 software (Molecular Device Inc.) through a Digidata 1332 A/D converter (Molecular Device Inc.) at a sampling rate of 20 point per ms. All target DNAs (D5, D16, and D30) and RNA (miR-155) were purchased from Integrated DNA technologies company, and applied to the *cis* chamber. Voltage was applied from the *trans* chamber. Current traces at voltage above +100 mV were not analyzed due to the channel's spontaneous current blocks[6]. Data were based on at least four separate experiments, and presented as mean ± standard deviation. The current amplitude histograms were fitted to the Gaussian distribution, and the block duration histograms were fitted

to the exponential distribution. The electrophysiology experiments were conducted at 22 ± 1 °C.

References

1. Kasianowicz, J.J. & Bezrukov, S.M. Protonation dynamics of the α-toxin ion channel from spectral analysis of pH-dependent current fluctuations. *Biophys. J.* **69**, 94-105 (1995).
2. Muthukumar, M. Theory of capture rate in polymer translocation. *The Journal of chemical physics* **132**, 195101 (2010).
3. Wanunu, M., Morrison, W., Rabin, Y., Grosberg, A.Y. & Meller, A. Electrostatic focusing of unlabelled DNA into nanoscale pores using a salt gradient. *Nature nanotechnology* **5**, 160-165 (2010).
4. Rowghanian, P. & Grosberg, A.Y. Electrophoretic capture of a DNA chain into a nanopore. *Physical Review E* **87**, 042722 (2013).
5. Wang, Y., Tian, K., Lehr, H., Ritzo, B. & Gu, L.-Q. Probing Molecular Pathways for DNA Orientational Trapping, Unzipping and Translocation in Nanopore by Using an Tunable Overhang Sensor. *Nanoscale* (2014).
6. Wang, Y. et al. Nanopore sensing of botulinum toxin type B by discriminating an enzymatically cleaved Peptide from a synaptic protein synaptobrevin 2 derivative. *ACS Appl Mater Interfaces* **7**, 184-192 (2015).
7. Shim, J.W., Tan, Q. & Gu, L.Q. Single-molecule detection of folding and unfolding of the G-quadruplex aptamer in a nanopore nanocavity. *Nucleic acids research* **37**, 972-982 (2009).